

Nuclear Shadowing and Antishadowing in a Unitarized BFKL Equation*

RUAN Jian-Hong, SHEN Zhen-Qi and ZHU Wei[†]

(Department of Physics, East China Normal University, Shanghai 200062, China)

Abstract

The nuclear shadowing and antishadowing effects are explained by a unitarized BFKL equation. The Q^2 - and x -variations of the nuclear parton distributions are detailed based on the level of the unintegrated gluon distribution. In particular, the asymptotical behavior of the unintegrated gluon distribution near the saturation limit in nuclear targets is studied. Our results in the nuclear targets are insensitive to the input distributions if the parameters are fixed by the data of a free proton.

PACS numbers: 13.60.Hb; 12.38.Bx.

keywords: nuclear shadowing and antishadowing; unintegrated gluon distribution in nuclei; QCD evolution equation

*Supported by National Natural Science Foundation of China 10135060, 10475028 and 10205004.

[†]Corresponding author, E-mail: weizhu@mail.ecnu.edu.cn

1 Introduction

The gluon distribution in the nuclear target is an essential ingredient in the calculation of high energy nuclear collisions, which relate to minijet production, dilepton production, heavy quarks and their bound states. Although the gluon density in a free nucleon was extracted by the experiments, however there are not enough data for the gluon distributions in nuclei. As well known the parton densities in a bound nucleon differ from in a free nucleon, the ratio of nuclear and deuterium structure functions is smaller or larger than unity at Bjorken variable $x < 0.05 - 0.1$ or $x \simeq 0.1 - 0.2$. These two facts are called the nuclear shadowing and antishadowing effects, respectively [1]. The understanding of nuclear shadowing and antishadowing in QCD is therefore an important issue to predict the nuclear gluon distributions. In this aspect, the parton recombination (fusion) between two different nucleons in a nucleus is a natural mechanism, which transfers the partons from a smaller x region to a larger x region and forms the nuclear shadowing and antishadowing effects [2].

The shadowing and antishadowing phenomena are also predicted to happen in a free nucleon: a rapid rise of parton multiplicities inside the proton at small x leads to the gluon recombination, which changes the distributions of gluon- and quark-densities, but does not change their total momenta. In consequence, a part of the gluon momentum lost in the shadowing should be compensated in terms of new gluons with larger x , which form the antishadowing. The modification of the gluon recombination to the standard DGLAP [3] evolution equation was first proposed by Gribov-Levin-Ryskin and Mueller-Qiu (the GLR-MQ equation) in [4], and it is naturally regarded as the QCD dynamics of the nuclear shadowing since the type of gluon fusion in a nucleon is still there in a nucleus but roughly differs by an $A^{1/3}$ scale [5]. However, the GLR-MQ equation does not predict the nuclear antishadowing effect since the momentum conservation in the gluon

recombination is violated in this equation. For this sake, a modified DGLAP equation was proposed to replace the GLR-MQ equation in [6,7], where the corrections of the gluon fusion to the DGLAP equation lead to the shadowing and antishadowing effects. Unfortunately, the integral solutions either in the GLR-MQ equation or in other modified DGLAP equations need the initial distributions on a boundary line (x, Q_0^2) at fixed Q_0^2 , and they contain the unknown input nuclear shadowing and antishadowing effects. Close, Qiu and Roberts [8] constructed a parton fusion model by QCD arguments and try to evolve the input parton distributions in the nuclear target, however, the results of this parton fusion model in the small x region are sensitive to the input parton distributions [9], which leads to a large uncertainty in the predictions. On the other hand, recently nuclear unintegrated gluon distribution becomes a useful and intuitive phenomenological language for applications to many high-energy nuclear collisions. However, the DGLAP equation and its modified forms are based on the collinear factorization scheme and they don't predict the evolution of the unintegrated parton distributions.

Instead of the above-mentioned modified DGLAP equations, an alternative QCD research for the nuclear shadowing and antishadowing is to modify the BFKL equation [10], which is directly written for the unintegrated gluon distribution. The evolutions of the BFKL-type equations are along the small x -direction: the input gluons distribute on the boundary line (x_0, \underline{k}^2) at fixed x_0 , where the gluon fusion begins, and *all* parton distributions both in a free nucleon and in a bound nucleon at $x < x_0$ are the evolution results of these equations. There are several nonlinear evolution equations considering the corrections of the gluon fusion to the BFKL evolution. One of the most widely studied models is the Balitsky-Kovchegov (BK) equation [11]. The BK equation is originally derived for the scattering amplitude in the transverse coordinator space. The nonlinear terms in the BK equation are formed by the dipole splitting and the screening effect origins from the

double scattering of the probe on the target. A remarkable solution of the BK equation is the so-called saturation, where the amplitude is a completely flat spectrum. However, the amplitude in the BK equation is re-normalized to identify the coefficient of the nonlinear term with that of the linear term. Therefore, the relation of the unintegrated gluon distribution with this scattering amplitude is unclear and it is model-dependent [12]. Besides, it is similar to the GLR-MQ equation, the BK equation is irrelevant to the antishadowing effect. Recently, a new modified BFKL equation incorporating the shadowing and antishadowing corrections of the gluon recombination to the unintegrated gluon distribution was proposed by Ruan, Shen, Yang and Zhu (the RSYZ equation) [13].

The purpose of this work is to explain the observed nuclear shadowing and antishadowing effects for the parton distributions using the RSYZ equation. The Q^2 - and x -variations of the nuclear parton distributions in the RSYZ equation are detailed in this work. Particularly, we predict the unintegrated nuclear gluon distributions using the RSYZ equation. The results show a logarithmic increasing spectral height, which is not identical to the prediction of the BK equation in the transverse coordinator space but is similar to a mean field result.

The paper is organized as follows. In Section 2 we give the RSYZ equation and its modifications in the nuclear target. The predictions of the RSYZ equation to the nuclear shadowing and antishadowing effects in the quark- and gluon-distributions as well as in the unintegrated gluon distributions are presented in Section 3.

2 The RSYZ evolution equation

The unintegrated gluon distribution f_N in a proton obeys the RSYZ evolution equation at small x [13], where the contributions of the gluon recombination to the BFKL dynamics are considered

$$\begin{aligned}
& -x \frac{\partial f_N(x, \underline{k}^2)}{\partial x} \\
& = \frac{\alpha_s N_c \underline{k}^2}{\pi} \int_{\underline{k}'^2_{min}}^{\infty} \frac{d\underline{k}'^2}{\underline{k}'^2} \left\{ \frac{f_N(x, \underline{k}'^2) - f_N(x, \underline{k}^2)}{|\underline{k}'^2 - \underline{k}^2|} + \frac{f_N(x, \underline{k}^2)}{\sqrt{\underline{k}^4 + 4\underline{k}'^4}} \right\} \\
& - \frac{36\alpha_s^2}{\pi \underline{k}^2 R^2} \frac{N_c^2}{N_c^2 - 1} f_N^2(x, \underline{k}^2) + \frac{18\alpha_s^2}{\pi \underline{k}^2 R^2} \frac{N_c^2}{N_c^2 - 1} f_N^2\left(\frac{x}{2}, \underline{k}^2\right), \quad x \leq x_0; \\
& -x \frac{\partial f_N(x, \underline{k}^2)}{\partial x} \\
& = \frac{\alpha_s N_c \underline{k}^2}{\pi} \int_{\underline{k}'^2_{min}}^{\infty} \frac{d\underline{k}'^2}{\underline{k}'^2} \left\{ \frac{f_N(x, \underline{k}'^2) - f_N(x, \underline{k}^2)}{|\underline{k}'^2 - \underline{k}^2|} + \frac{f_N(x, \underline{k}^2)}{\sqrt{\underline{k}^4 + 4\underline{k}'^4}} \right\} \\
& + \frac{18\alpha_s^2}{\pi \underline{k}^2 R^2} \frac{N_c^2}{N_c^2 - 1} f_N^2\left(\frac{x}{2}, \underline{k}^2\right), \quad x_0 \leq x \leq 2x_0, \tag{1}
\end{aligned}$$

where $R = 1 \text{ fm}$ (or $< 1 \text{ fm}$) if the gluons are uniformly distributed in a nucleon (or the gluons are located in the hot-spots); x_0 is the starting point of the gluon fusions. Note that the shadowing and antishadowing coexist in the region $x \leq x_0$, while there is only the antishadowing in $x_0 \leq x \leq 2x_0$ [14].

We should point out that the nonlinear terms in Eq. (1) are really from the evolution kernel of the MD-DGLAP equation [6], where the double logarithmic approximation is taken, i.e., both the x and transverse momenta are strongly ordered. Obviously, this approximation satisfies such x -region, where the values of x are not extra small. On the other hand, the linear terms of Eq. (1) are the BFKL-kernel, which works in the small x range. The mix of two approximations in Eq. (1) is feasible for the discussions of the nuclear shadowing and antishadowing effects, since they occupy the transition range

from a middle x to small x . The RSYZ is directly derived for the unintegrated gluon distribution, which relates to the (integrated) gluon distribution using

$$G_N(x, Q^2) \equiv x g_N(x, Q^2) = \int_{\underline{k}_{min}^2}^{Q^2} \frac{d\underline{k}^2}{\underline{k}^2} f_N(x, \underline{k}^2). \quad (2)$$

Since the density of gluons increases rapidly with decreasing x , the sea quark distributions are increasingly dominated by the gluon distribution, via the DGLAP splitting $G \rightarrow q\bar{q}$. Thus, the deep inelastic structure function at small x reads [15]

$$\begin{aligned} & F_{2N}(x, Q^2) \\ &= 2 \int_x^1 dx_1 \int^{Q^2} \frac{d\underline{k}^2}{\underline{k}^2} \int^{\underline{k}^2} \frac{d\underline{k}'^2}{\underline{k}'^2} f_N\left(\frac{x}{x_1}, \underline{k}'^2\right) \sum_q e_q^2 \frac{\alpha_s}{2\pi} P_{qG}(x_1). \end{aligned} \quad (3)$$

where $P_{qG}(x_1)$ is the DGLAP splitting function.

Now we discuss the RSYZ equation in the nuclear target. The gluons with smaller x exceed the longitudinal size of nucleon in a nucleus. We assume that the gluons inside the nucleus are completely overlapping and fusion along the longitudinal momentum direction at the evolution starting point x_0 . Thus, the strength of the nonlinear recombination terms in Eq. (1) should be scaled by $A^{1/3}$ in a nucleus. On the other hand, although the softer gluons of different nucleons with extra small \underline{k}^2 may be correlated on the transverse plane because the integrations on \underline{k}^2 can go down to a very small value in Eq. (1), we neglect these corrections due to $f_N(x, \underline{k}^2 \rightarrow 0) \rightarrow 0$. In this simple model the RSYZ equation in the nucleus becomes

$$\begin{aligned} & -x \frac{\partial f_A(x, \underline{k}^2)}{\partial x} \\ &= \frac{\alpha_s N_c \underline{k}^2}{\pi} \int_{\underline{k}_{min}^2}^{\infty} \frac{d\underline{k}'^2}{\underline{k}'^2} \left\{ \frac{f_A(x, \underline{k}'^2) - f_A(x, \underline{k}^2)}{|\underline{k}'^2 - \underline{k}^2|} + \frac{f_A(x, \underline{k}^2)}{\sqrt{\underline{k}^4 + 4\underline{k}'^4}} \right\} \\ & - A^{1/3} \frac{36\alpha_s^2}{\pi \underline{k}^2 R^2} \frac{N_c^2}{N_c^2 - 1} f_A^2(x, \underline{k}^2) + A^{1/3} \frac{18\alpha_s^2}{\pi \underline{k}^2 R^2} \frac{N_c^2}{N_c^2 - 1} f_A^2\left(\frac{x}{2}, \underline{k}^2\right), \quad x \leq x_0; \end{aligned}$$

$$\begin{aligned}
& -x \frac{\partial f_A(x, \underline{k}^2)}{\partial x} \\
& = \frac{\alpha_s N_c \underline{k}^2}{\pi} \int_{\underline{k}'^2_{min}}^{\infty} \frac{d\underline{k}'^2}{\underline{k}'^2} \left\{ \frac{f_A(x, \underline{k}'^2) - f_A(x, \underline{k}^2)}{|\underline{k}'^2 - \underline{k}^2|} + \frac{f_A(x, \underline{k}^2)}{\sqrt{\underline{k}^4 + 4\underline{k}'^4}} \right\} \\
& \quad + A^{1/3} \frac{18\alpha_s^2}{\pi \underline{k}^2 R^2} \frac{N_c^2}{N_c^2 - 1} f_A^2\left(\frac{x}{2}, \underline{k}^2\right), \quad x_0 \leq x \leq 2x_0.
\end{aligned} \tag{4}$$

The distributions $G_A(x, Q^2)$ and $F_{2A}(x, Q^2)$ in the nucleus are computed by using the equations corresponding to Eqs. (2) and (3).

3 Numerical analysis and summary

We use a parameter form of a BFKL-like solution as the input distribution [13] at $2x_0 = 0.3$

$$f_N(2x_0, \underline{k}^2) = f_A(2x_0, \underline{k}^2) = \beta \sqrt{\underline{k}^2} \frac{x_0^{-\lambda_{BFKL}}}{\sqrt{\ln \frac{1}{x_0}}} \exp\left(-\frac{\ln^2(\underline{k}^2/1 \text{ GeV}^2)}{2\lambda' \ln(1/x_0)}\right), \quad (5)$$

where $\lambda_{BFKL} = 12\alpha_s/(\pi \ln 2)$ and β and λ' are two parameters.

The computations of the RSYZ equation need pre-know the value of $f_{N(A)}(x_i/2, \underline{k}^2)$ at the step $x = x_i$. For this sake, we proposed the following program in [13]

$$f_{N(A)}\left(\frac{x_i}{2}, \underline{k}^2\right) = f_{N(A), \text{Shadowing}}\left(\frac{x_i}{2}, \underline{k}^2\right) + \frac{f_{N(A), BFKL}\left(\frac{x_i}{2}, \underline{k}^2\right) - f_{N(A), \text{Shadowing}}\left(\frac{x_i}{2}, \underline{k}^2\right)}{i\eta - \eta + 1}, \quad (6)$$

where $f_{N(A), \text{Shadowing}}(x_i/2, \underline{k}^2)$ (or $f_{N(A), BFKL}(x_i/2, \underline{k}^2)$) indicates that the evolution from x_i to $x_i/2$ is controlled by Eq. (1) but without the antishadowing contributions (or is controlled by the BFKL equation). The parameter η implies the different velocities approaching the BK dynamics. We temporarily take $\eta = \infty$ and we will indicate it is appropriate.

At first, we use the well known $F_{2N}(x, Q^2)$ -data [16] of a free proton to determine the parameters in the computations. Then we predict the distributions in nuclei. In this work we fix the coupling constant to be $\alpha_s = 0.3$. The dashed curve in Fig. 1 is our fitting result using $\beta = 7.22$, $\lambda' = 0.002$ and $R = 2.6 \text{ GeV}^{-1}$. Note that the contributions from the valence quarks to F_2 at $x > 0.1$ are necessary and they can be parameterized by the difference between the dashed curve and the experimental solid curve in Fig. 1.

Figure 2 shows the predictions of the RSYZ equation for the Ca/C, Ca/Li, Ca/D and Cu/D compared with the EMC and NMC results [17,18]. The agreement is acceptable.

Figure 3 indicates that the enhancement in the Sn gluon distribution with respect to that in C observed by NMC [19] is consistent with our predictions.

No significant Q^2 -dependence on the ratios of the structure functions at small x has been concluded in the present experimental precision. However, it does not prevent us exposing the possible Q^2 -variations of the nuclear shadowing, which may be hidden in the larger experimental errors. The ratios $G_{Ca}(x, Q^2)/G_D(x, Q^2)$ for gluon distributions at $Q^2 = 2$ and 10 GeV^2 using Eqs. (1) and (2) are given in Fig.4a. The Q^2 -variations of the gluon ratios are predicted in the region $10^{-4} < x < 10^{-1}$ in our model. The logarithmic slope b in $G_A/G_{A'} = a + b \ln Q^2$ is positive. However, the corresponding slope in the ratio of the structure functions F_{2Ca}/F_{2D} is negative (see Fig.4b). For example, the predicted Q^2 -slope for calcium at $x \simeq 4 \times 10^{-2}$, $b \simeq -0.046$, and at $x \simeq 10^{-2}$, $b \simeq -0.03$, the results are compatible with the measured data in [20]. A more significant Q^2 -dependence of the structure function ratios can be found in the heavy nucleus F_{2Xe}/F_{2D} . A flatter ratio at $x < 10^{-2}$ in the E665 data [21] was presented. However, it can't be understood as the saturation behavior, where the parton fusion balances the parton splitting. The reason is that the parton densities in the proton still increase toward the small x -direction at $x < 0.01$ (see Fig.1). Alternatively, we consider that this behavior is a consequence of the Q^2 -variations of the structure function ratios since the experimental point with the smaller x corresponds to the smaller value of Q^2 in Fig. 5.

An important parameter in the computing RSYZ equation is η in Eq. (5). The observed nuclear shadowing and antishadowing provide an example to determine the value of η . The results incline to a minimum antishadowing, i. e., $\eta = \infty$.

Comparing with the modified DGLAP equation, the RSYZ equation directly predicts the nuclear unintegrated gluon distributions, which are important information for the researches of high energy nuclear collisions. We compute the unintegrated gluon distribu-

tions in different nuclear targets using the RSYZ equation. In Fig. 6 we plot the spectra of the gluon density on the transverse momentum squared $dG/d\underline{k}^2 \equiv dG/dQ^2|_{Q^2=\underline{k}^2} = f(x, \underline{k}^2)/\underline{k}^2 \sim \underline{k}^2$. The BK equation on the transverse coordinator space predict the saturation solutions, where the amplitude is a completely flat spectrum at $\underline{k}^2 < Q_s^2(x)$, and the spectral height is irrelevant to the values of x (i.e., the geometric scaling); $Q_s^2(x)$ is the saturation scale. The saturation limit and the geometric scaling are expected to appear in the larger nucleus, where the shadowing effects are enhanced. However, the logarithmic increasing spectral height in our results is not identical to this prediction of the BK equation but is similar to the mean field result: $dG/d\underline{k}^2 \propto \ln(Q_s^2(x)/\underline{k}^2)$ [22].

Finally, we discuss the dependence of our solutions with the input distributions. For this sake, we change the parameters in Eq. (24) to: $\beta = 0.15$, $\lambda' = 9.64$, $R = 2.4 \text{ GeV}^{-1}$ and strongly distort the input form. Then we repeat our calculating programs. We find that the results are insensitive to the input distributions.

In summary, the nuclear shadowing and antishadowing effects are explained by a unitarized BFKL equation. The Q^2 - and x -variations of the nuclear parton distributions are detailed based on the level of the unintegrated gluon distribution. In particular, the asymptotical behavior of the unintegrated gluon distribution in various nuclear targets is studied. We find that the geometric scaling in the expected saturation range is violated. Our results in the nuclear targets are insensitive to the input distributions if the parameters are fixed by the data of a free proton. We believe that these results are useful in studying the ultrarelativistic heavy ion collisions.

References

- [1] Arneodo M. Phys. Rept., 1994, 240: 301-393
- [2] Nikolaev N N, Zakharov V I. Phys. Lett., 1975, B55:397-399
- [3] Altarelli G, Parisi G. Nucl. Phys., 1977, B126: 298-318; Gribov V N, Lipatov L N. Sov. J. Nucl. Phys., 1972, 15: 438-450; Dokshitzer Y L. Sov. Phys. JETP., 1977, 46: 641-653
- [4] Gribov L V, Levin E M and Ryskin M G. Phys. Rept., 1983, 100: 1-150; Mueller A H, Qiu J. Nucl. Phys., 1986, B268: 427-452
- [5] Qiu J W. Nucl. Phys., 1987, B291: 746-764; Eskola K J, Qiu J W and Wang X N. Phys. Rev. Lett., 1994, 72: 36-39; Eskola K J, Honkanen H, Kolhinen V J, Qiu J W and Salgado C A. Nucl. Phys., 2003, B660: 211-224
- [6] ZHU Wei. Nucl. Phys., 1999, B551: 245-274
- [7] ZHU Wei, RUAN Jian-Hong, Yang Ji-Feng and SHEN Zhen-Qi, Phys. Rev., 2003, D68: 094015.
- [8] Close F E, Qiu J W and Roberts R G. Phys. Rev., 1989, D40: 2820-2831.
- [9] Kumano S, Phys.Rev., 1993, C48: 2016-; Phys.Lett., 1993, B298: 171-175
- [10] Lipatov L N. Sov. J. Nucl. Phys., 1976, 23: 338-345; Fadin V S, Kuraev E.A. and Lipatov L N. Phys. Lett., 1975, B60: 50-52; Kuraev E A, Lipatov L N and Fadin V S, Sov. Phys. JETP., 1976, 44: 443-450; Kuraev E A, Lipatov L N and Fadin V S. Sov. Phys. JETP., 1977, 45: 199-204; Balitsky I I, Lipatov L N. Sov. J. Nucl. Phys., 1978, 28: 822-829

- [11] Balitsky I. Nucl. Phys., 1996, B463:99-; Kovchegov Yu. Phys. Rev., 1999, D60:034008; Phys. Rev., 2001, D61:074018.
- [12] Kutak K, Stasto A M. Eur.Phys.J., 2005, C41: 343-351.
- [13] RUAN Jian-Hong, SHEN Zhen-Qi, YANG Ji-Feng and Zhu Wei. Nucl. Phys., 2007, B760: 128-144.
- [14] ZHU Wei, XUE Da-Li, CHAI Kang-Ming and XU Zai-Xin. Phys. Lett., 1993, B317: 200-204; ZHU Wei, CHAI Kang-Ming and HE Bo. Nucl. Phys., 1994, B427: 525-533; ZHU Wei, CHAI Kang-Ming and HE Bo. Nucl. Phys., 1995, B449: 183-196
- [15] Askew A J, Kwiecinski J, Martin A D and Sutton P J. Phys. Rev., 1993, D47: 3775-3782
- [16] Derrick M et al. Zeit.Phys., 1996, C72: 399-424; Benvenuti A C et al. Phys. Lett., 1989, B223: 485-489
- [17] CERN NA28/EMC, Arneodo M et al. Phys. Lett., 1988, B211: 493-499 ; Nucl. Phys., 1990, B333: 1-47
- [18] CERN NA37/NMC, Amaudruz P et. al. Nucl. Phys., 1995, B441: 3-11
- [19] CERN NA37/NMC, Amaudruz P et. al., Nucl. Phys., 1992, B371: 553-566
- [20] Bodek A (SLAC E139), talk at the Lepton-Photon Symposium and Europhysics Conference on High Energy Physics LP-HEP91, Geneva, Switzerland, 25th July-1st August 1991.
- [21] FNAL E665, Adams M R et al. Phys. Rev. Lett., 1992, 68: 3266-3269
- [22] Iancu E, A. Leonidov, and L. McLerran, hep-ph/0202270, and references therein.

Figure Captions

Fig. 1 The fit of the computed $F_{2P}(x, Q^2 = 10 \text{ GeV}^2)$ in proton by the RSYZ equation using the input Eq. (5) (dashed curve). The contributions of the valence quarks are parameterized by the differences between solid and dashed curves. The data are taken from [16].

Fig. 2 Predictions of the RSYZ equation compared with the ratios of the structure functions for various nuclei. The data are taken from [17,18]. All curves are for $Q^2 = 10 \text{ GeV}^2$

Fig. 3 Predictions for the ratio of the gluon distributions in Sn/C . The curve is the result of the RSYZ equation for $Q^2 = 10 \text{ GeV}^2$ and the data are taken from [19].

Fig. 4 (a) Q^2 -dependence of the ratios for the gluon distributions Ca/D in the RSYZ equation. (b) Similar to (a) but for the structure functions.

Fig. 5 Q^2 -dependence of the ratios for the structure functions Xe/D in the RSYZ equation. The data are taken from [21].

Fig. 6 Predicted spectrum $dG/d\underline{k}^2 = f(x, \underline{k}^2)/\underline{k}^2$ on the \underline{k}^2 -space in various nuclear targets in the RSYZ equation. Dotted curves $x = 10^{-5}$, dashed curves $x = 10^{-6}$ and solid curves $x = 10^{-7}$.

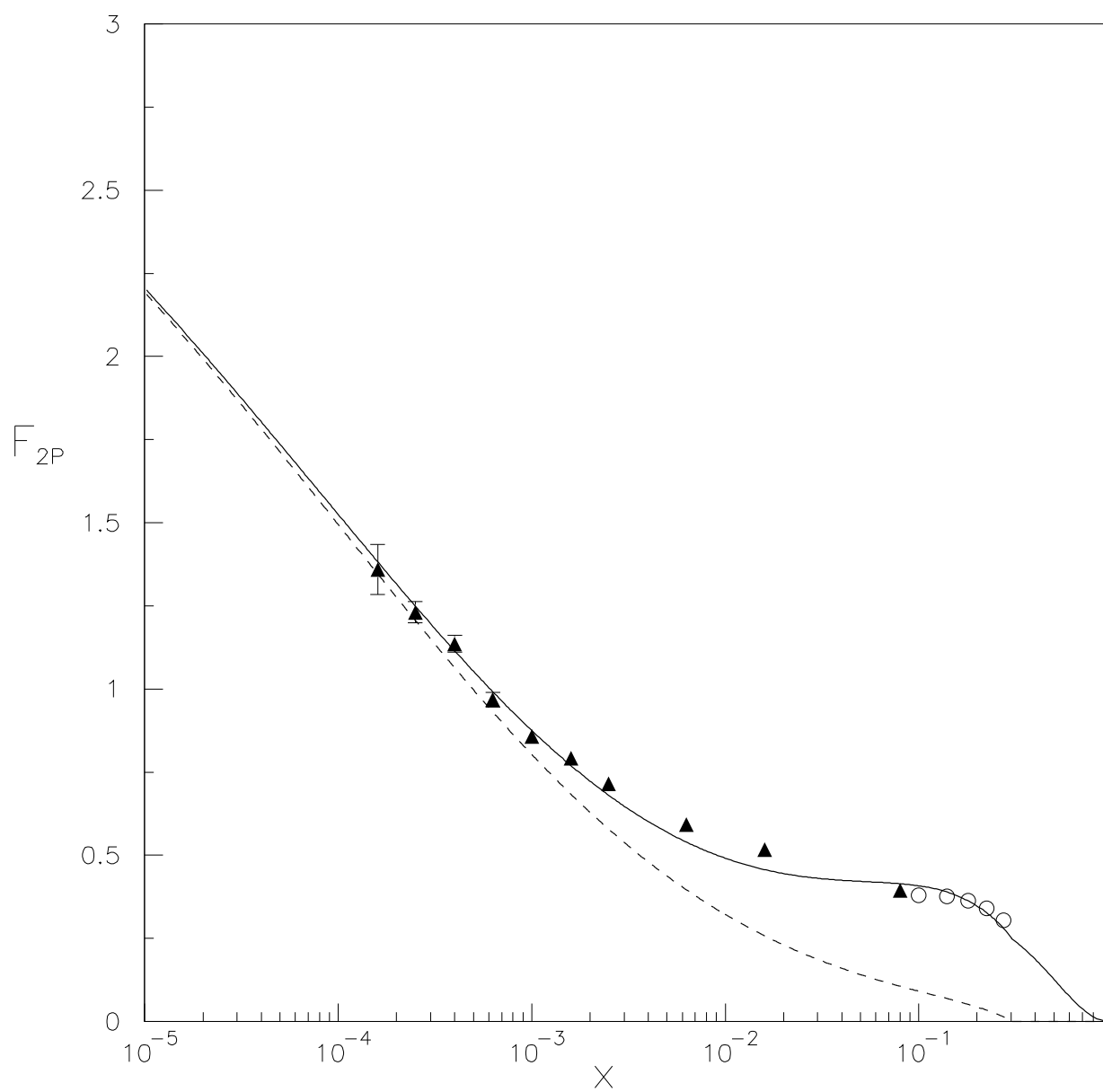


Fig.1

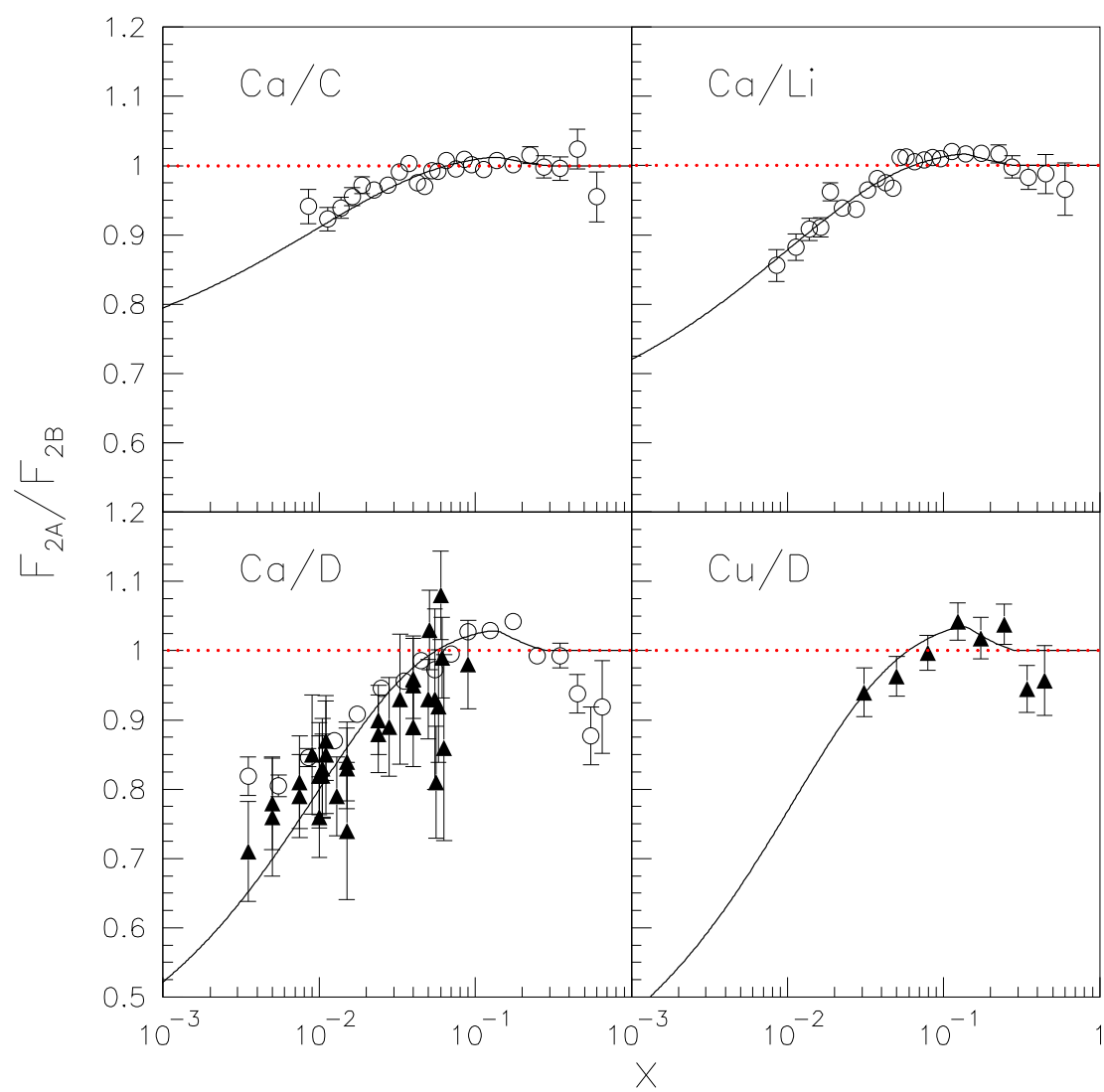


Fig.2

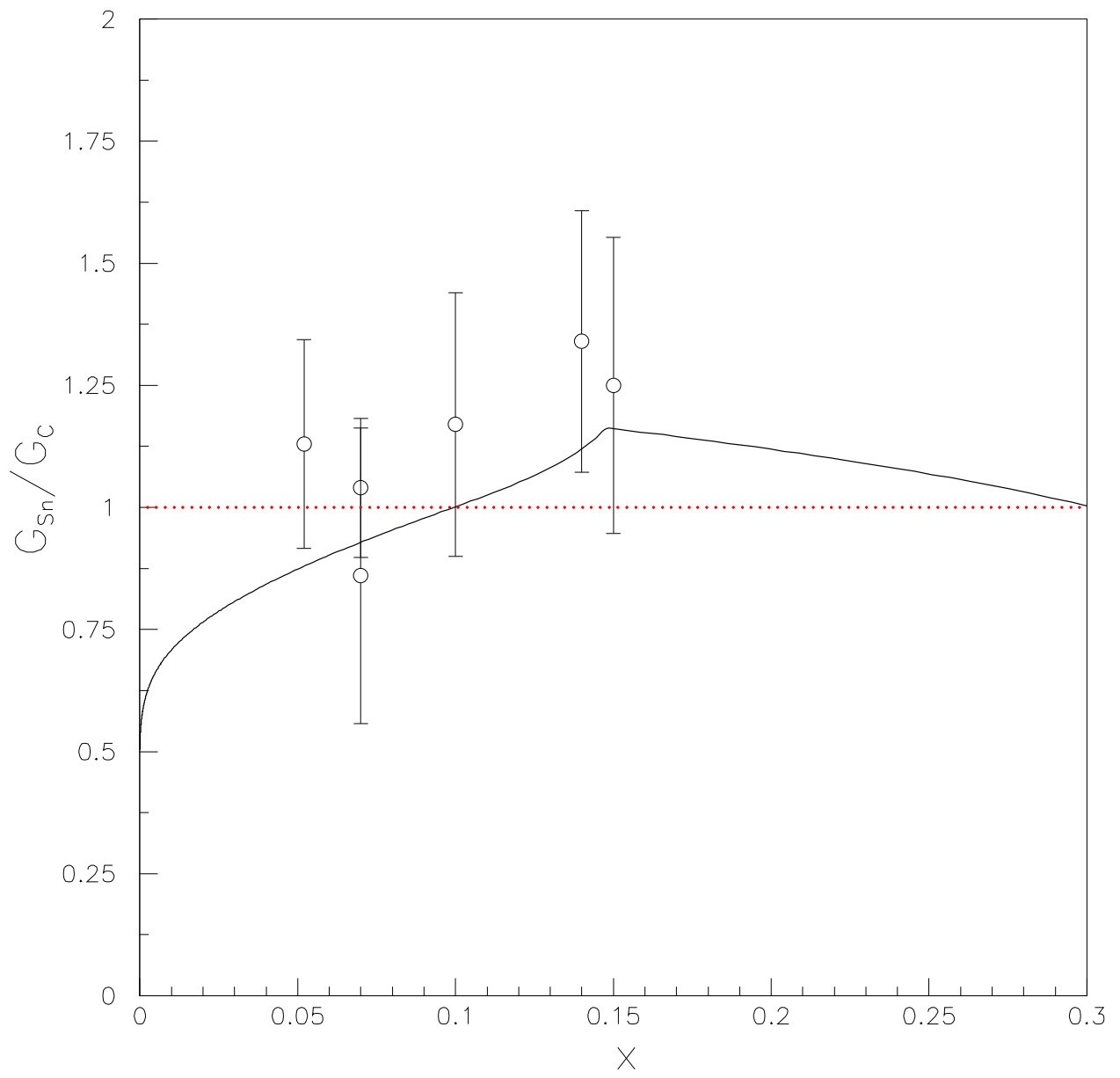


Fig.3

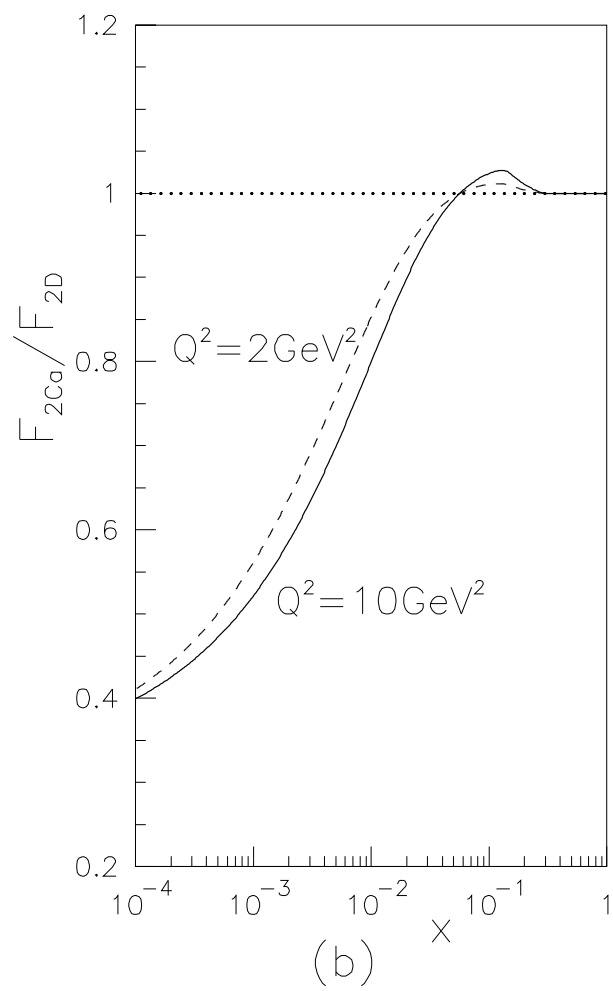
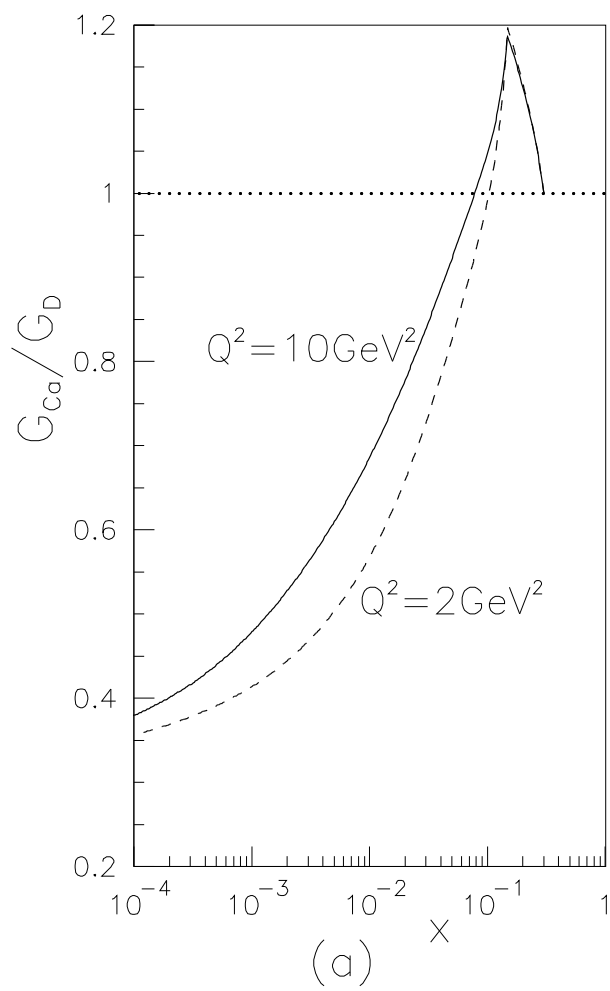


Fig.4

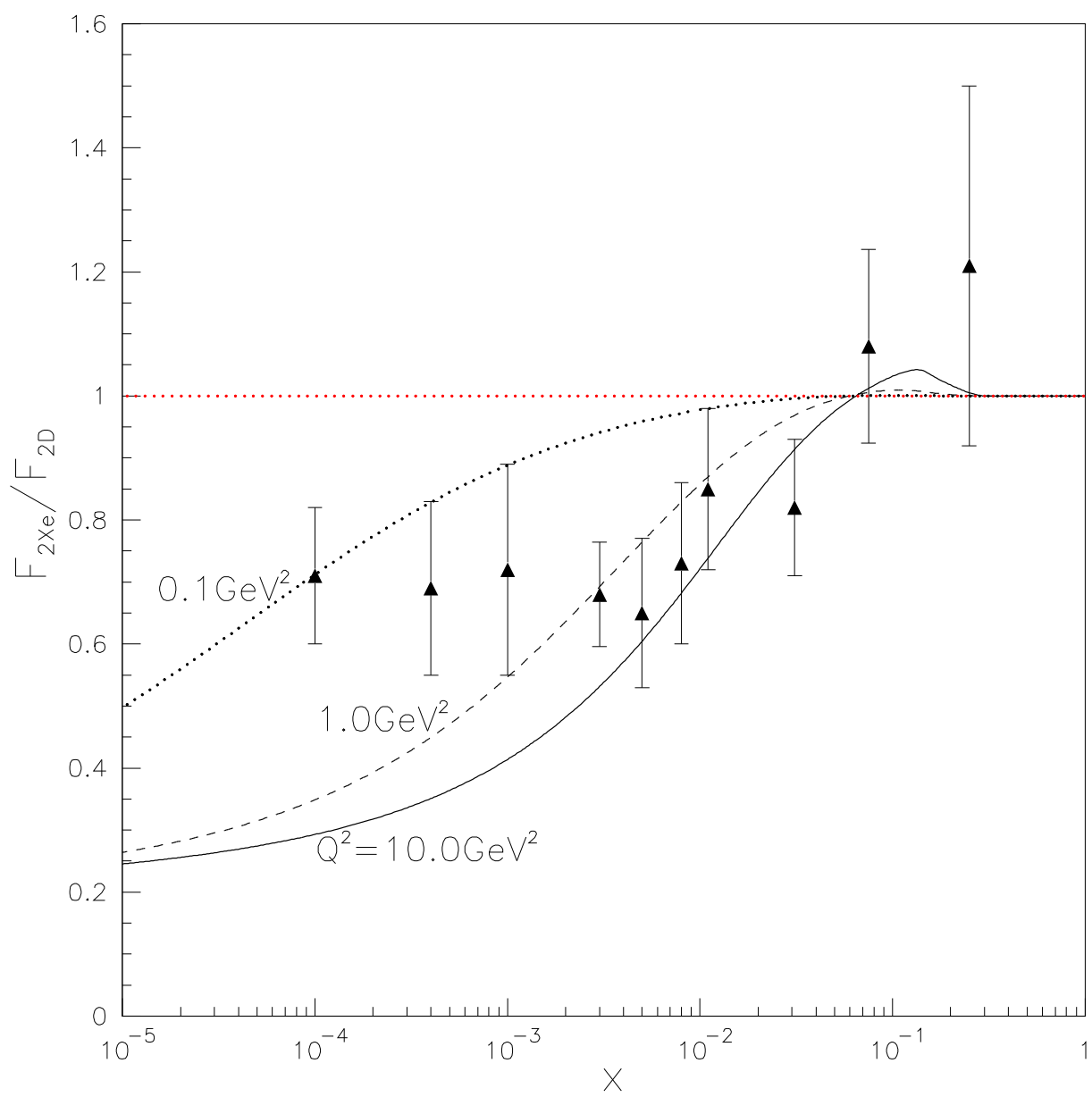


Fig.5

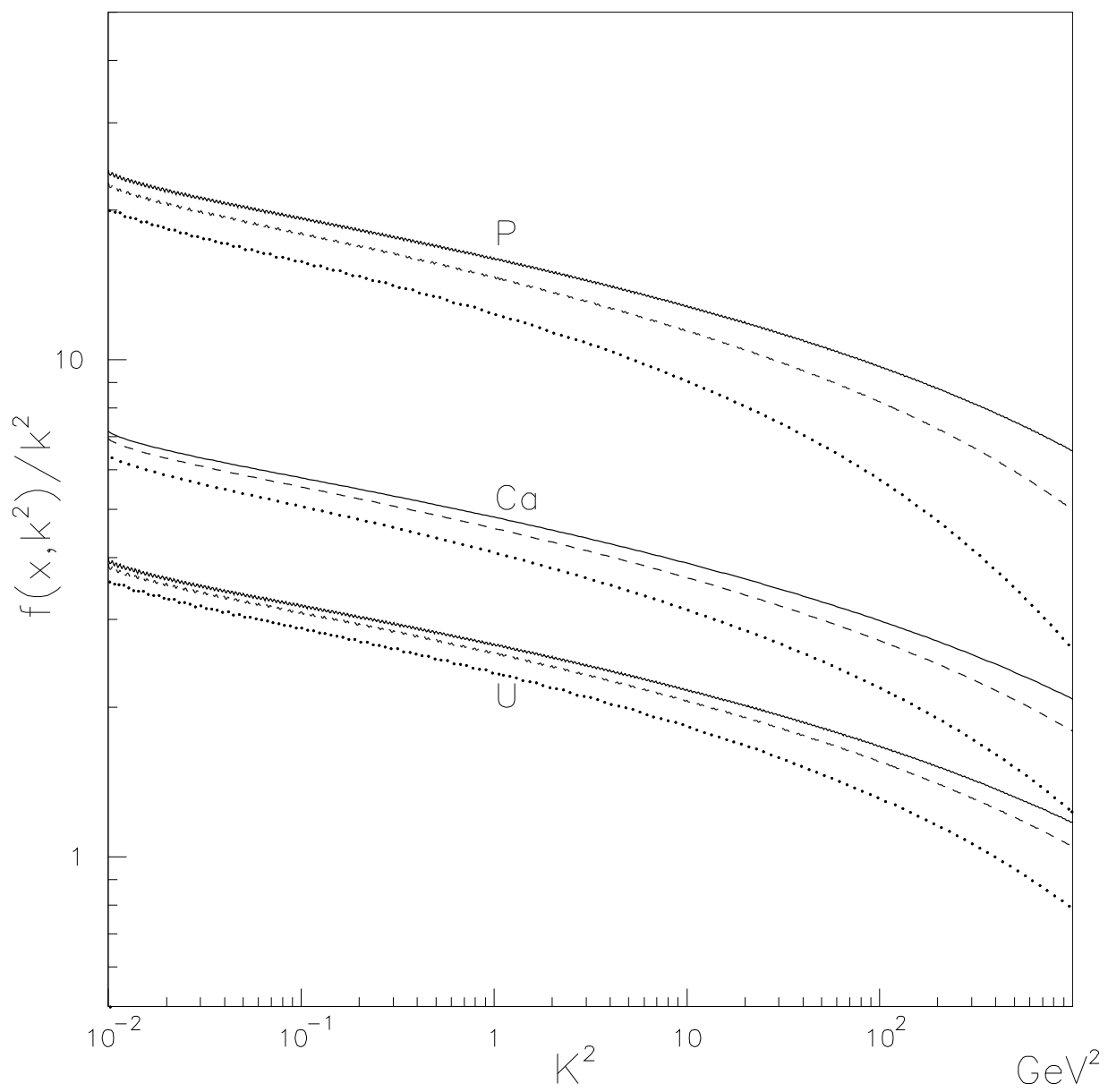


Fig.6